DALTON

Complexes of silver(I), thallium(I), lead(II) and barium(II) with bis[3-(2-pyridyl)pyrazol-1-yl]phosphinate: one-dimensional helical chains and discrete mononuclear complexes

Elefteria Psillakis, John C. Jeffery, Jon A. McCleverty* and Michael D. Ward*

School of Chemistry, University of Bristol, Cantock's Close, Bristol BS8 1TS, UK

Reaction of 3-(2-pyridyl)pyrazole with $POBr_3$ in toluene–NEt_3 afforded not the expected tris(pyrazolyl)phosphine oxide but the partially hydrolysed compound bis[3-(2-pyridyl)pyrazol-1-yl]phosphinate (as its triethylammonium salt). This compound has two potentially chelating N,N′-bidentate arms linked by an apical PO_2^- group. Reaction with $AgNO_3$, $Tl(O_2CMe)$, $Pb(NO_3)_2$ or $Ba(NO_3)_2$ in dry MeCN followed by recrystallisation afforded crystals of the complexes $[AgL]\cdot 2H_2O$, $[TlL]\cdot MeOH$, $[PbL_2]\cdot H_2O$ and $[(BaL_2)_3]\cdot 6MeCN\cdot 2H_2O$ respectively, all of which have been crystallographically characterised. The compound $[AgL]\cdot 2H_2O$ contains infinite helical chains $(AgL)_\infty$ in which each ligand donates one N,N′-bidentate arm to each of two metals and each metal ion is four-co-ordinated by two arms from different ligands. The strands are held together in the crystal by a complex network of hydrogen bonds involving lattice water molecules and also by aromatic π-stacking interactions. The compound $[TlL]\cdot MeOH$ is likewise a one-dimensional helical polymer of TlL units, with each ligand bridging two metals and each Tl ion in a '2 + 3' co-ordination geometry with two short bonds to ligands (<2.71 Å) and three longer, weak bonds (>2.87 Å): there is an obvious gap in the co-ordination sphere due to a stereochemically active lone pair. A combination of interstrand aromatic π-stacking interactions and hydrogen-bonding interactions involving the lattice MeOH molecule is present. The compound $[PbL_2]\cdot H_2O$ is in contrast a discrete mononuclear complex, four-co-ordinated just by one bidentate arm from each of the two ligands with the other bidentate arms pendant: again there is a stereochemically active lone pair. The metal geometry is approximately trigonal bipyramidal with the lone pair in an equatorial position. The lattice water molecule is hydrogen bonded to three different complex units. The compound $[(BaL_2)_3]\cdot 6MeCN\cdot 2H_2O$ contains mononuclear BaL_2 and dinuclear Ba_2L_4 units: the former is ten-co-ordinate, with each ligand acting as an N_4O donor and a phosphinate oxygen atom participating in co-ordination, whereas in the latter each Ba^{II} is nine-co-ordinated and two of the ligands are bridging, donating their four N atoms to one metal ion and a phosphinate oxygen atom to the other.

The relationship between the steric and electronic preferences of the metal ions and the co-ordinating properties of the ligand, and how these interact to control self-assembly processes and determine the structures of complexes, is of fundamental interest in supramolecular and co-ordination chemistry.[1] In this context many ligands which contain two bidentate compartments linked by a flexible bridge are known and their inherent flexibility means that they can adapt to the specific preferences of different metal ions in different ways.[2–6] Often they form dinuclear helical complexes,[2] but can co-ordinate in other ways if the stereoelectronic preferences of different metal ions demands it.[3] A good example of this flexible co-ordination behaviour is provided by 2,2′:6′,2″:6″,2‴-quaterpyridine and its derivatives, which can form dinuclear double helicates with Cu^I and Ag^I[4] but also co-ordinate in a planar tetradentate manner to metals which prefer square-planar or octahedral geometry.[5] Other tetradentate ligands show similar behaviour.[6]

Use of metal ions which have no stereoelectronic geometric preferences arising from partially filled d shells allows examination of the possible co-ordination modes of a ligand in the absence of metal-directed requirements. We describe here the preparation of a simple bridging anion $[L]^-$ containing two bidentate binding sites linked by a phosphinate bridge, which forms infinite one-dimensional single-stranded helical structures with Ag^I and Tl^I but discrete mononuclear complexes with Pb^{II} and Ba^{II}. The anion and all of the complexes have been crystallographically characterised.

Experimental

Syntheses

(*a*) Trimethylammonium bis[3-(2-pyridyl)pyrazol-1-yl]phosphinate $[NEt_3H][L]$. To a solution of 3-(2-pyridyl)pyrazole[7] (5.45 g, 37.6 mmol) and dry triethylamine (5.0 g, 50 mmol) in dry toluene (40 cm^3) maintained between 0 and 5 °C was added dropwise a solution of $POBr_3$ (3.6 g, 12.5 mmol) in dry toluene (10 cm^3) with constant stirring. The mixture was stirred at room temperature for 1 h and then heated to reflux for 10 h. After cooling, the mixture was filtered to remove NEt_3HBr and the filtrate concentrated *in vacuo*, upon which a precipitate appeared. This was filtered off and dried; cooling of the remaining mother-liquor overnight afforded an additional crop of the product, which was finally recrystallised from MeCN–diethyl ether. Yield: 70% (Found: C, 57.2; H, 6.2; N, 21.2. Calc. for $C_{22}H_{28}N_7O_2P\cdot 0.5Et_2O$: C, 57.3; H, 6.1; N, 21.2%). ^{1}H NMR [$(CD_3)_2CO$, 300 MHz]: δ 8.55 (2 H, ddd, J = 4.5, 1.6, 1.0, pyridyl H^6), 8.16 (2 H, dd, J = 2.3, 0.5, pyrazolyl H^5), 7.95 (2 H, d, J = 7.2, pyridyl H^3), 7.76 (2 H, td, J = 6.9, 1.6, pyridyl H^4), 7.25 (2 H, ddd, J = 6.8, 4.4, 1.1, pyridyl H^5) and 6.89 (2 H, t, J = 2.2 Hz, pyrazolyl H^4). ν(P=O) (KBr disc) 1167 cm^{-1}.

(*b*) AgL. A mixture of $[NEt_3H][L]$ (0.45 g, 1.0 mmol) and $AgNO_3$ (0.17 g, 1.0 mmol) in dry MeCN (8 cm^3) was agitated in an ultrasound bath for 20 min. A white precipitate appeared which was filtered off, washed several times with MeCN and dried to give the product in 70% yield. X-Ray-quality crystals were grown by slow evaporation of a $CHCl_3$ solution of the material (Found: C, 40.3; H, 2.6; N, 17.0. Calc. for $C_{16}H_{12}AgN_6O_2P\cdot 0.2CHCl_3$: C, 40.3; H, 2.5; N, 17.4%). ν(P=O) (KBr disc) 1168 cm^{-1}.

(*c*) TlL. This was prepared and isolated in the same way as the silver complex above, from $[NEt_3H][L]$ (0.21 g, 0.47 mmol) and thallium(I) acetate (0.12 g, 0.47 mmol) in dry MeCN (10

cm^3). The yield of the resulting white precipitate of TlL was 82%. X-Ray-quality crystals were grown by slow evaporation of a methanol or dichloromethane solution of the material (Found: C, 32.7; H, 2.1; N, 14.1. Calc. for $C_{16}H_{12}N_6O_2PTl\cdot 0.5CH_2Cl_2$: C, 33.1; H, 2.1; N, 14.1%). FAB mass spectrum: $m/z = 557$ (40, TlL), 761 (100, Tl_2L) and 1316 (10%, Tl_2L_3). ν(P=O) (KBr disc) 1168 cm^{-1}.

(*d*) PbL_2. This was prepared and isolated in the same way as the silver complex above, from $[NEt_3H][L]$ (0.23 g, 0.50 mmol) and $Pb(NO_3)_2$ (0.17 g, 0.50 mmol) in dry MeCN (10 cm^3). The yield of the resulting white precipitate of PbL_2 was 98%. X-Ray-quality crystals were grown by slow evaporation of a concentrated CH_2Cl_2 solution of the material (Found: C, 41.3; H, 2.9; N, 18.3. Calc. for $C_{32}H_{24}N_{12}O_4P_2Pb\cdot H_2O$: C, 41.3; H, 2.8; N, 18.1%). FAB mass spectrum: m/z = 559 (100, PbL), 910 (15, PbL_2) and 933 (8%, PbL_2 + Na). ν(P=O) (KBr disc) 1168 and 1184 cm^{-1}.

(*e*) BaL_2. This was prepared and isolated in the same way as the silver complex above, from $[NEt_3H][L]$ (0.11 g, 0.25 mmol) and $Ba(NO_3)_2$ (0.065 g, 0.25 mmol) in dry MeCN (10 cm^3). The yield of the resulting white precipitate of BaL_2 was 73%. X-Ray-quality crystals were grown by slow evaporation of a concentrated MeCN solution of the material (Found: C, 43.7; H, 2.7; N, 19.4. Calc. for $C_{32}H_{24}BaN_{12}O_4P_2\cdot H_2O$: C, 44.8; H, 3.0; N, 19.6%). FAB mass spectrum m/z = 489 (100, BaL) and 841 (20%, BaL_2). ν(P=O) (KBr disc) 1171 cm^{-1}.

Crystallography

Suitable crystals were quickly transferred from the mother-liquor to a stream of cold N_2 at −100 °C on a Siemens SMART diffractometer fitted with a CCD-type area detector. A detailed experimental description of the methods used for data collection and integration using the SMART system has been published.[8] Table 1 contains a summary of the crystal parmeters, data collection and refinement. In all cases the structures were solved by conventional heavy-atom or direct methods and refined by the full-matrix least-squares method on all F^2 data using the SHELXTL 5.03 package[9] on Silicon Graphics Indigo-R4000 or Indy computers. In all cases, non-hydrogen atoms were refined with anisotropic thermal parameters; hydrogen atoms were included in calculated positions and refined with isotropic thermal parameters.

The compound AgL crystallises with two molecules of water per complex formula unit. Each asymmetric unit contains 1.5 formula units, *i.e.* $[AgL]_{1.5}\cdot 3H_2O$. There is one complete Ag atom per asymmetric unit, with a second located on a C_2 axis. One of the pyridyl rings [atoms N(61), C(62)–C(66)], although co-ordinated, is disordered over two slightly different orientations. Atom C(62), which is the position of attachment of the pyrazolyl ring, is common to both components of the disorder but the other five atoms were successfully separated into two components (which were restrained to be similar) in the ratio 53:47. Only the major component is shown in the Figures.

The structural determination of [TlL]·MeOH was well behaved and presented no problems.

In $[PbL_2]\cdot H_2O$, three of the ligand carbon atoms [C(43), C(44) and C(64)] had unusually high thermal parameters ($U_{eq} > 0.1$ Å^2). However attempts to split these atoms into disordered components (as in $[AgL]\cdot 2H_2O$, above) were unsuccessful.

Crystals of $[(BaL_2)_3]\cdot 6MeCN\cdot 2H_2O$ diffracted weakly so data were collected to $2\theta = 46.5°$, rather than 55° which was the limit for the others; however the structure solution and refinement presented no particular problems. The structure is actually $[(BaL_2)(Ba_2L_4)]\cdot 6MeCN\cdot 2H_2O$, containing a mononuclear BaL_2 fragment and a dinuclear Ba_2L_4 fragment, both of which lie astride inversion centres.

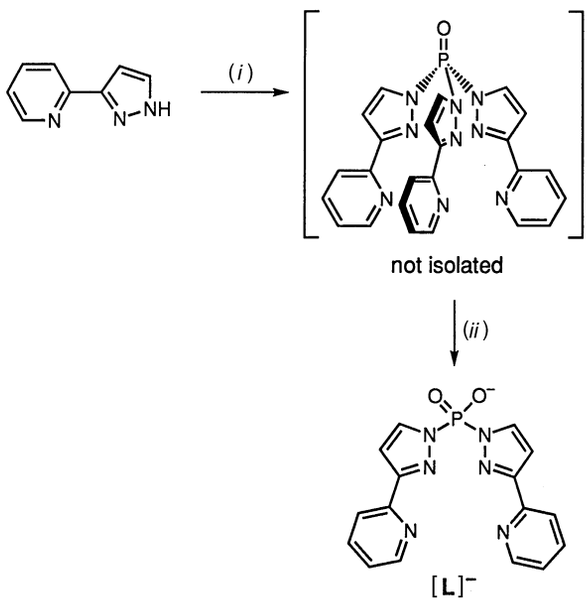

Scheme 1 (*i*) $POBr_3$, toluene, NEt_3, reflux; (*ii*) moisture

Atomic co-ordinates, thermal parameters, and bond lengths and angles have been deposited at the Cambridge Crystallographic Data Centre (CCDC). See Instructions for Authors, *J. Chem. Soc., Dalton Trans.*, 1997, Issue 1. Any request to the CCDC for this material should quote the full literature citation and the reference number 186/442.

Results and Discussion

Ligand synthesis and crystal structure

Reaction of 3,5-dimethylpyrazole (Hdmpz) with $POBr_3$ has been previously reported to yield the tris(pyrazol-1-yl)-phosphine oxide $(dmpz)_3P{=}O$, which acts as a facial tridentate ligand similar in its co-ordination behaviour to a tris(pyrazolyl)borate.[10] It was found to be prone to partial hydrolysis to give the bis(pyrazol-1-yl)phosphinate $[(dmpz)_2PO_2]^-$ which could co-ordinate as an N,N,O-donor terdentate ligand.[10,11] We performed the reaction of 3-(2-pyridyl)pyrazole (HR) with $POBr_3$ and NEt_3 to try and prepare the hexadentate podand $R_3P{=}O$ in which three bidentate pyridylpyrazolyl arms are linked at the apical P=O group, in a comparable manner to the hexadentate podand $[R_3BH]^-$ which we have studied extensively recently.[8,12] Instead partial hydrolysis occurred during the synthesis or work-up to give the bis(pyrazol-1-yl)phosphinate $[NEt_3H][R_2PO_2]$ (the anion of which is hereafter referred to as L^-; Scheme 1). The P=O stretching band in the IR spectrum of the product was at a rather low frequency for a phosphine oxide and the elemental analysis indicated formation of $[NEt_3H]$-$[R_2PO_2]$ rather than $R_3P{=}O$. This happened despite the use of 'dry' reagents, probably during the work-up and recrystallisation when the reaction mixture was handled in air. In subsequent syntheses no special precautions were taken to exclude moisture during work-up and purification, so that $[NEt_3H]$-$[R_2PO_2]$ could be prepared deliberately.

The formulation of the material was confirmed by X-ray analysis (Fig. 1, Table 2). Each bidentate arm has a transoid conformation, with the pyridyl ring being twisted by 8° with respect to the plane of the adjacent pyrazolyl ring in each case. The two molecules in the unit cell are associated by a weak C–H · · · N hydrogen-bonding interaction across the inversion centre, with the C · · · N separation being 3.42 Å. There is a much stronger N–H · · · O hydrogen-bonding interaction between the $[NEt_3H]^+$ cation and one of the phosphinate oxygen atoms, with the N · · · O separation being 2.70 Å. The geometry about each phosphorus atom is rather distorted from tetra-

Table 1 Summary of crystal parameters, data collection and refinement for the five new compounds

	$[NEt_3H][L]$	$[AgL]_{1.5}\cdot 3H_2O$	$[TlL]\cdot MeOH$	$[PbL_2]\cdot H_2O$	$[BaL_2]\cdot[Ba_2L_4]\cdot 6MeCN\cdot 2H_2O$
Formula	$C_{22}H_{28}N_7O_2P$	$C_{24}H_{24}Ag_{1.5}N_9O_6P_{1.5}$	$C_{17}H_{16}N_6O_3PTl$	$C_{32}H_{26}N_{12}O_5P_2Pb$	$C_{108}H_{94}Ba_3N_{42}O_{14}P_6$
M	453.48	742.78	587.70	927.78	2802.09
System, space group	Triclinic, $P\bar{1}$	Monoclinic, $C2/c$	Triclinic, $P\bar{1}$	Triclinic, $P\bar{1}$	Triclinic, $P\bar{1}$
a/Å	8.9275(14)	13.930(3)	8.3653(12)	7.8328(12)	10.663(3)
b/Å	10.997(3)	24.258(4)	8.598(2)	11.263(2)	14.729(4)
c/Å	13.916(3)	17.670(2)	13.869(2)	20.800(6)	20.674(9)
α/°	94.751(11)	—	99.540(9)	83.17(2)	100.27(2)
β/°	105.663(13)	97.670(8)	100.627(9)	81.50(3)	101.54(4)
γ/°	112.23(2)	—	96.684(14)	70.398(11)	107.18(3)
U/Å^3	1191.2(4)	5917(2)	955.7(3)	1704.9(6)	2940(2)
Z	2	8	2	2	1
D_c/g cm^{-3}	1.264	1.668	2.042	1.807	1.583
μ/mm^{-1}	0.148	1.138	8.566	5.103	1.156
F(000)	480	2976	560	908	1406
Crystal size/mm	0.70 × 0.10 × 0.05	0.30 × 0.25 × 0.20	0.60 × 0.25 × 0.15	0.25 × 0.10 × 0.05	0.25 × 0.15 × 0.05
2θ Range for data collection/°	3–55	3–55	3–55	4–55	3–46.5
Reflections collected (total, independent, R_{int})	7570, 5196, 0.025	18 751, 6735, 0.041	6110, 4193, 0.030	11 096, 7578, 0.043	10 518, 7890, 0.067
Data, restraints, parameters	5194, 0, 296	6735, 209, 444	4193, 0, 255	7575, 0, 477	7881, 0, 779
Final $R1$, $wR2$ [a,b]	0.043, 0.110	0.041, 0.095	0.021, 0.055	0.051, 0.105	0.062, 0.111
Weighting factors (a, b) [b]	0.0311, 0.84	0.0428, 0.83	0.0318, 1.41	0, 14.65	0.0166, 0
Largest peak, hole/e Å^{-3}	+0.241, −0.364	+0.897, −1.230	+0.718, −1.046	+0.855, −1.383	+0.641, −0.704

[a] Structure was refined on F_o^2 using all data; the value of $R1$ is given for comparison with older refinements based on F_o with a typical threshold of $F \geqslant 4\sigma(F)$. [b] $wR2 = [\Sigma w(F_o^2 - F_c^2)^2/\Sigma w(F_o^2)^2]^{\frac{1}{2}}$ where $w^{-1} = [\sigma^2(F_o^2) + (aP)^2 + bP]$ and $P = [\max(F_o^2, 0) + 2F_c^2]/3$.

Table 2 Selected bond lengths (Å) and angles (°) for the anion of $[NEt_3H][L]$

P(1)–O(2)	1.4647(13)	N(11)–C(15)	1.361(2)
P(1)–O(1)	1.4795(13)	N(11)–N(12)	1.367(2)
P(1)–N(11)	1.724(2)	N(12)–C(13)	1.330(2)
P(1)–N(31)	1.727(2)	C(21)–N(22)	1.334(2)
		N(22)–C(23)	1.341(2)
O(2)–P(1)–O(1)	125.13(8)	O(2)–P(1)–N(31)	106.06(8)
O(2)–P(1)–N(11)	110.07(7)	O(1)–P(1)–N(31)	107.40(7)
O(1)–P(1)–N(11)	104.39(7)	N(11)–P(1)–N(31)	101.35(7)

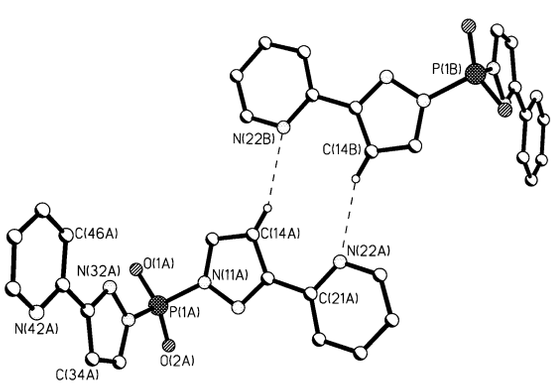

Fig. 1 Crystal structure of the anion in $[NEt_3H][L]$, showing the weak hydrogen bonding leading to association of two anions across an inversion centre

hedral, with the O–P–O angle being 125° and the other angles being correspondingly slightly compressed. Otherwise the structure has no unusual features.

One-dimensional helical polymers with Ag^I and Tl^I

Reaction of $[NEt_3H][L]$ with $AgNO_3$ in dry MeCN afforded a white precipitate the elemental analyses of which were consistent with a 1:1 metal:ligand stoichiometry (and retention of some of the solvent of crystallisation). Ligands with two or more bidentate N-donor compartments commonly assemble around Cu^I or Ag^I to give oligonuclear double helicates in which the metal ions are in a pseudo-tetrahedral geometry,[1,2,13]

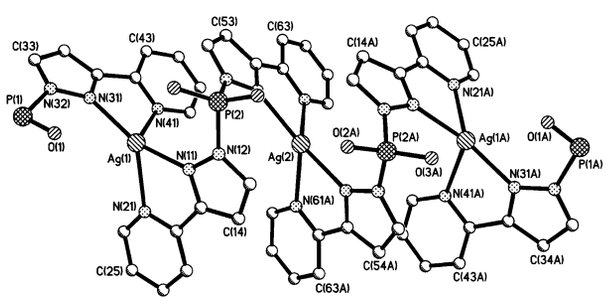

Fig. 2 Crystal structure of the one-dimensional helical chain of $[AgL]\cdot 2H_2O$

and we consequently thought that a simple double helix Ag_2L_2 would be the most likely structure for this complex.

The crystal structure of $[AgL]\cdot 2H_2O$ (Fig. 2, Table 3) shows that the complex is indeed helical, but is also an infinite one-dimensional polymer. Each Ag^+ ion is as expected in a four-co-ordinate environment, arising from two bidentate N,N-chelating arms from two separate ligands, with the Ag–N distances lying in the range 2.211–2.520 Å [apart from Ag(2)–N(61B) in the minor disordered component which is 2.63 Å]. Each ligand therefore bridges two metal ions. However instead of formation of a discrete 2:2 helical complex which would require the two ligands to be 'in register' with each other, each ligand is 'slipped' with respect to the adjacent ligands to give an infinite chain. The asymmetric unit contains one unique silver atom [Ag(1)] and another half atom on a C_2 axis [Ag(2)]. The sequence of silver atoms along the chain is therefore . . . 1–2–1–1–2–1 . . . with the structure repeating after every three silver atoms; there are C_2 axes through Ag(2) and midway between the two equivalent adjacent Ag(1) atoms. The Ag(1)···Ag(1′) and Ag(1)···Ag(2) distances are 6.857 and 5.450 Å respectively. There are interligand aromatic stacking interactions (3.2–3.6 Å) both within each helical strand and between strands. This is a common feature of helical complexes[1] but one which is not essential for helicate formation:[14] the matching of metal-ion co-ordination geometry and ligand donor properties is probably more important.

A consequence of the ligand arrangement is that all of the anionic phosphinate groups lie in a line along one face of the strand, such that each infinite helical strand has polar and non-

Table 3 Selected bond lengths (Å) and angles (°) for [AgL]·2H_2O

Ag(1)–N(31)	2.211(3)	Ag(1)–N(21)	2.406(3)
Ag(1)–N(11)	2.252(3)	Ag(1)–N(41)	2.515(3)
Ag(2)–N(61A)[a]	2.238(13)[b]	Ag(2)–N(61B′)	2.631(12)[c]
Ag(2)–N(61A′)	2.238(13)[b]	Ag(2)–N(52)	2.288(3)
Ag(2)–N(61B)	2.631(12)[c]	Ag(2)–N(52′)	2.288(3)
N(31)–Ag(1)–N(11)	156.18(10)	N(31)–Ag(1)–N(41)	70.21(10)
N(31)–Ag(1)–N(21)	131.63(10)	N(11)–Ag(1)–N(41)	114.08(10)
N(11)–Ag(1)–N(21)	71.67(10)	N(21)–Ag(1)–N(41)	102.15(10)
N(61A′)–Ag(2)–N(61A)	83.0(10)[b]	N(52)–Ag(2)–N(61B′)	135.3(3)[c]
N(61A′)–Ag(2)–N(52)	130.9(4)[b]	N(52′)–Ag(2)–N(61B′)	66.4(3)[c]
N(61A)–Ag(2)–N(52)	75.8(4)[b]	N(52)–Ag(2)–N(61B)	66.4(3)[c]
N(61A′)–Ag(2)–N(52′)	75.8(4)[b]	N(52′)–Ag(2)–N(61B)	135.3(3)[c]
N(61A)–Ag(2)–N(52′)	130.9(4)[b]	N(61B′)–Ag(2)–N(61B)	110.5(5)[c]
N(52)–Ag(2)–N(52′)	148.35(14)		

[a] For the atoms co-ordinated to Ag(2) the prime denotes a symmetry-related atom; thus N(61A) and N(61A′) are related by a C_2 operation. The suffixes A and B denote the two different disordered components of the pyridyl ring N(61), C(62)–C(66) which was disordered over two orientations. [b] Major component of disorder (57%). [c] Minor component of disorder (43%).

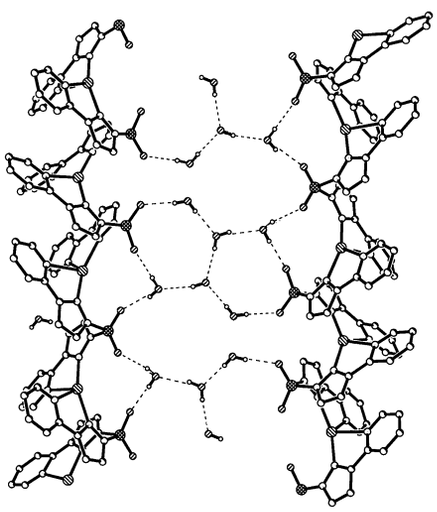

Fig. 3 Association of chains in [AgL]·2H_2O *via* a hydrogen-bonding network involving the phosphinate groups and lattice water molecules

polar faces. This results in two types of interstrand association in the crystal, which can be called 'face-to-face' and 'back-to-back', illustrated in Figs. 3 and 4. The two polar faces of adjacent strands are associated *via* a complicated network of hydrogen bonding involving the phosphinate oxygen atoms and water molecules (Fig. 3). Some of the water hydrogen atoms were disordered so this depiction of the hydrogen-bonding network is necessarily somewhat arbitrary, but it illustrates clearly the interstrand cross-linking assisted by the water molecules. In the 'back-to-back' association (Fig. 4) the non-polar faces of two adjacent strands are together, resulting in an interleaved 'herring-bone' type of pattern in which T-stacking edge-to-face interactions between the strands are apparent. The structure is therefore stabilised by both inter- and intra-strand π-stacking interactions as well as the interstrand hydrogen bonding. Interestingly the complex was recrystallised from $CHCl_3$, although the solvent was not predried and the solution was left to stand in air: the presence of trace quantities of moisture is obviously of fundamental importance for the formation of these crystals.

Reaction of [NEt_3H][L] with thallium(I) acetate in dry MeCN leads to a white precipitate the elemental analytical and mass spectroscopic data of which again indicated a 1:1 formulation, *i.e.* TlL. The crystal structure of [TlL]·MeOH is shown in Fig. 5. Again the complex is an infinite one-dimensional chain, simi-

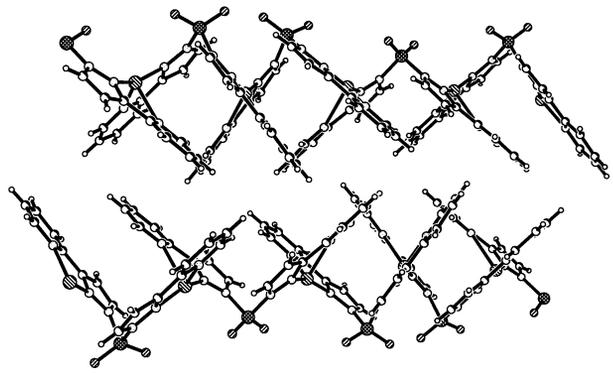

Fig. 4 Interaction between the two hydrophobic faces of the helical chains in [AgL]·2H_2O

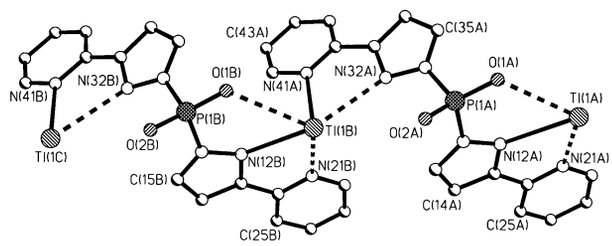

Fig. 5 Crystal structure of the one-dimensional helical chain of [TlL]·MeOH. The metal ions are all crystallographically equivalent

lar to that of AgL. The co-ordination geometry is difficult to describe, as there is a wide spread of bond lengths from the Tl^{I} to various donor atoms, covering the range 2.68–3.08 Å (Table 4).

In thallium(I) complexes with tris(pyrazolyl)borate ligands the metal ion is in a three-co-ordinate pyramidal geometry with Tl–N distances of 2.5–2.7 Å and there is a stereochemically active lone pair occupying the 'vacant' site of the tetrahedral co-ordination sphere.[15–17] If other potential donor atoms are also present[15,16] these tend to interact more weakly, with Tl–L separations of above 3 Å. The primary co-ordination geometry is therefore trigonal pyramidal, with additional long-range interactions when required. In TlL there is no such clear demarcation between 'strong' and 'weak' co-ordinate bonds. In Fig. 5 the two shortest Tl–N interactions to N(41) and N(12) (2.68 and 2.71 Å respectively) are indicated by solid lines, as these correspond to the distances of 'strong' bonds observed in other complexes.[15–17] The three longer interactions [to N(21), N(32) and O(1); 2.872, 2.956 and 3.087 Å respectively] are indicated as dashed lines; the gap in the co-ordination sphere, occupied by the stereochemically active lone pair, is clear.

Fig. 6 shows the crystal packing of the helical chains. It is clear that both face-to-face (separation *ca.* 3.7 Å) and edge-to-face stacking interactions between aromatic rings occur. There is also weak hydrogen bonding between the phosphinate oxygen atoms of one chain [O(1)] and the C–H hydrogen atoms H(35) of another chain and H(44) of a third chain, with O···H distances of 2.45 and 2.37 Å respectively. In addition there are methanol solvent molecules in the lattice (one per Tl atom) which are involved in three hydrogen-bonding interactions as both donor and acceptor (Fig. 7), thereby acting as a bridge between two chains in the same way as the water molecules in the structure of the silver(I) complex described earlier. The methanol OH interacts with the phosphinate oxygen atom O(2) of one chain (non-bonded O···O separation 2.71 Å) and the methanol oxygen atom simultaneously acts as a hydrogen-bond acceptor from two CH hydrogen atoms of a different chain [C(23) and C(25); non-bonded O···C separations 3.42 and 3.36 Å respectively]. This structure is therefore similar to that of [AgL]·2H_2O in that one-dimensional helical chains are formed which are stabilised in the crystal by both inter- and

Table 4 Selected bond lengths (Å) and angles (°) for [TlL]·MeOH

Tl(1)–N(41A)	2.682(3)	Tl(1)–N(21)	2.872
Tl(1)–N(12)	2.709(3)	Tl(1)–N(32A)	2.956
		Tl(1)–O(1)	3.087
N(41A)–Tl(1)–N(12)	82.06(8)	N(12)–Tl(1)–N(32A)	139.1
N(41A)–Tl(1)–N(21)	77.7	N(12)–Tl(1)–O(1)	59.2
N(41A)–Tl(1)–N(32A)	59.8	N(21)–Tl(1)–N(32A)	96.3
N(41A)–Tl(1)–O(1)	83.9	N(21)–Tl(1)–O(1)	116.9
N(12)–Tl(1)–N(21)	58.7	N(32A)–Tl(1)–O(1)	124.4

Parameters which have no calculated estimated standard deviations involve atoms that were considered by the software to be beyond normal bonding distance; they were calculated from the final atomic coordinates after refinement.

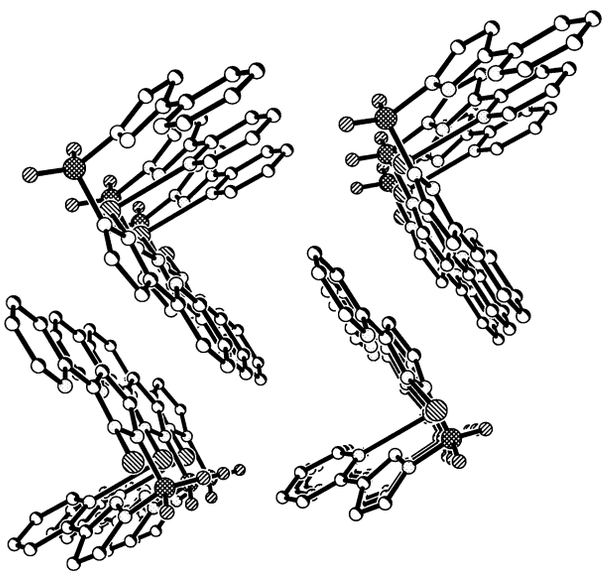

Fig. 6 Crystal packing of the helical chains in [TlL]·MeOH

intra-strand π stacking and by inter- and intra-strand hydrogen bonding *via* solvent molecules.

Helicates have become widespread in co-ordination chemistry in the last decade as interest has grown in self-assembly methods to prepare large, high-nuclearity structures with sophisticated molecular architectures that are unattainable by more conventional synthetic methods.[1,2] The majority of such complexes are discrete double or triple helicates containing a small number of metal centres, usually two or three. Considerably rarer are infinite one-dimensional helical structures,[18] which arise (as here) when the bridging ligands are 'slipped' relative to one another and which are of particular interest not just for the self-assembly processes which produce them, but also because of their striking anisotropy which may find applications in the areas of one-dimensional conductors ('molecular wires') or new magnetic materials. Discrete mononuclear complex units may also give rise to one-dimensional helical chains, not through bridging ligands, but through association in such a way that the component parts are twisted slightly with respect to one another in the same sense along the 'axis of assembly', such that helicity arises.[19] These types of co-ordination polymer may be contrasted with the polymeric structures that arise from dinucleating bridging ligands with a 'back-to-back' arrangement of binding sites.[20]

Discrete mononuclear complexes with Pb^{II} and Ba^{II}

The reaction of $[NEt_3H][L]$ with $Pb(NO_3)_2$ afforded in near-quantitative yield a material with elemental analysis and FAB mass spectrum indicating the formulation PbL_2. Two views of the crystal structure of $[PbL_2]\cdot H_2O$ are in Figs. 8 and 9 and

Table 5 Selected bond lengths (Å) and angles (°) for $[PbL_2]\cdot H_2O$

Pb–N(81)	2.539(6)	Pb–N(32)	2.638(6)
Pb–N(41)	2.613(6)	Pb–N(72)	2.692(6)
N(81)–Pb–N(41)	77.9(2)	N(81)–Pb–N(72)	64.3(2)
N(81)–Pb–N(32)	83.0(2)	N(41)–Pb–N(72)	80.1(2)
N(41)–Pb–N(32)	63.8(2)	N(32)–Pb–N(72)	135.8(2)

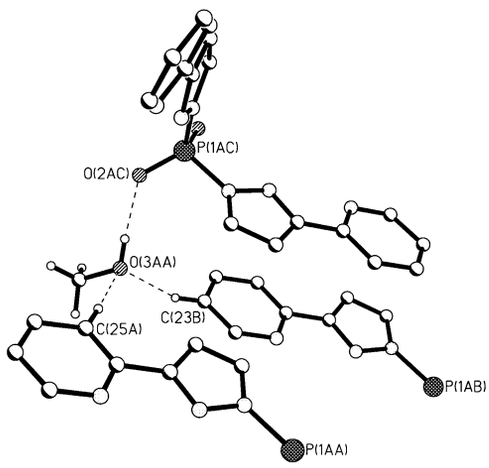

Fig. 7 Hydrogen-bonding interactions involving the solvent MeOH and adjacent stacked chains in [TlL]·MeOH

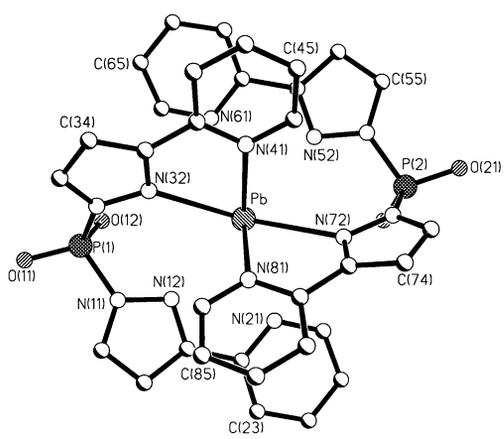

Fig. 8 Crystal structure of $[PbL_2]\cdot H_2O$

show that, in contrast to the complexes of Ag^{I} and Tl^{I}, PbL_2 is a simple mononuclear complex albeit one with some unusual features. As with the thallium(I) complex, the description of the co-ordination geometry is not straightforward because of the presence of a wide range of metal–donor atom separations (2.54–3.11 Å). However these are fairly clearly split into two sets of four, with one set of four short bonds (2.54–2.69 Å), (Table 5) and four long bonds (2.85–3.11 Å). Comparison with the crystal structures of other lead(II) complexes shows that this is common behaviour,[16,21] and that the lead(II) ion is best considered here as basically four-co-ordinate with four additional long, weak interactions. Each ligand has one bidentate arm co-ordinated to the metal centre with one arm 'pendant' but still weakly interacting with the metal.

In Figs. 8 and 9 therefore only the four shorter interactions are shown as bonds and it is clear from Fig. 9 in particular that the lone pair of the Pb^{II} is stereochemically active. The four co-ordinated N atoms occupy very approximately the two axial sites and two of the three equatorial sites of a trigonal bipyramid. This geometric description is limited by the non-ideal bite angles of the bidentate arms and the other steric constraints inherent in the structure [for example, the 'axial' pair of

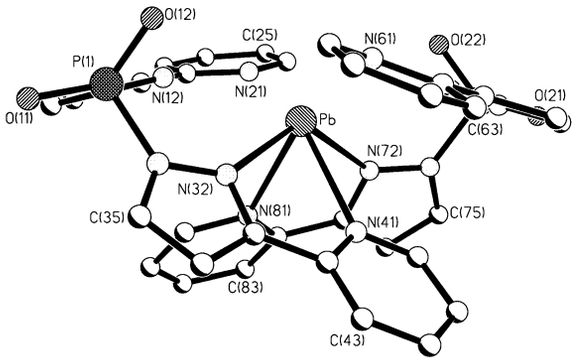

Fig. 9 Alternative view of the crystal structure of $[PbL_2]\cdot H_2O$, emphasising the presence of pendant ligand arms and the stereochemically active lone pair

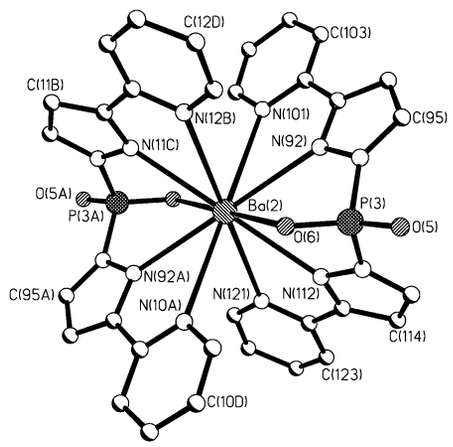

Fig. 10 Crystal structure of the BaL_2 fragment of $[(BaL_2)_3]\cdot 6MeCN\cdot 2H_2O$

atoms N(32) and N(72) subtend an angle of 135.8° at the Pb] but seems to be preferable to the alternative extreme of square-pyramidal geometry. The geometry about the Pb^{II} is similar to that observed in $[Pb(HBR_3)(NO_3)]$ [HR = 3-(2-pyridyl)pyrazole].[16] The disposition of the two pendant arms is interesting. They are approximately planar, with the lone pairs of the potentially co-ordinating nitrogen atoms cisoid and facing inwards towards the metal, rather than transoid as would be expected for electronic reasons if the pendant arm were not interacting with the metal.[22] However these lone pairs are not pointed directly towards the metal ion, but point to the space 'above' it (Fig. 9) which is occupied by the metal lone pair. The interaction of the pendant groups with the metal is therefore strong enough to ensure that these donor atoms point approximately inwards but not strong enough to make them point exactly at the metal centre and this vindicates the decision to treat these four interactions as of secondary importance.

The lattice water molecule is involved in both donor and acceptor hydrogen-bonding interactions involving different complex units. It acts as a hydrogen-bond donor (O^w–H · · · O^p, where w denotes water and p phosphinate) to two phosphinate oxygen atoms of different complex units [O(11) from one unit and O(12) from the second], with O · · · O separations of 2.79 and 2.80 Å respectively. The water oxygen atom also acts as a hydrogen-bond acceptor, forming a weak C–H · · · O interaction (C · · · O 3.14 Å) with H(86) with a third complex unit. The lattice water molecule therefore plays an important role in determining the crystal packing.

The reaction of $[NEt_3H][L]$ with $Ba(NO_3)_2$ afforded in good yield a material with elemental analysis and FAB mass spectrum indicating the formulation BaL_2. Crystallisation from MeCN afforded crystals of $[(BaL_2)_3]\cdot 6MeCN\cdot 2H_2O$ the structure of which (Figs. 10 and 11) is surprisingly complicated. The unit cell contains independent mononuclear (BaL_2, Fig. 10) and

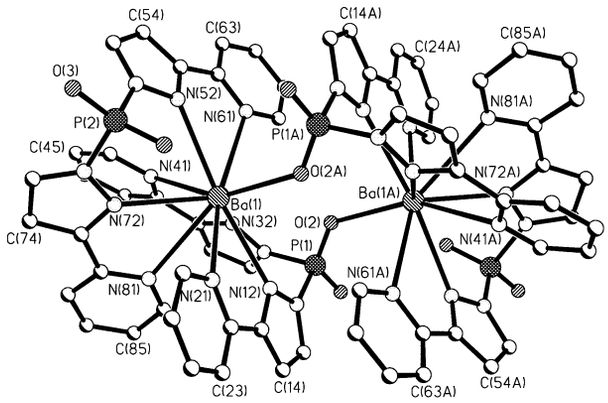

Fig. 11 Crystal structure of the Ba_2L_4 fragment of $[(BaL_2)_3]\cdot 6MeCN\cdot 2H_2O$

dinuclear (Ba_2L_4, Fig. 11) units, both of which lie astride inversion centres; *i.e.* the asymmetric unit contains half of the monomer and half of the dimer, giving the overall formulation $[(BaL_2)(Ba_2L_4)]\cdot 6MeCN\cdot 2H_2O$ for the crystalline material. We see here that the phosphinate oxygen atoms can co-ordinate under the appropriate conditions.[10,11] Thus, the monomer $[BaL_2]$ is ten-co-ordinate with an N_8O_2 donor set and each ligand pentadentate. In the dimer $[Ba_2L_4]$ each Ba^{II} is nine-co-ordinate with an N_8O donor set from one tetradentate (N_4) ligand and one pentadentate (N_4O) ligand the four N atoms of which are co-ordinated to one metal ion whilst the O is co-ordinated to the second one. The two pentadentate ligands are therefore bridging, allowing formation of the $[Ba_2L_4]$ dimer. The bond distances (Table 6) are in the normal range for barium complexes.[23] Interestingly, the lengths of the Ba–O bonds in the mononuclear complex unit BaL_2 (both 3.14 Å) are significantly longer than that in the dinuclear complex unit Ba_2L_4 (2.73 Å). This is a reflection of the electroneutrality principle: in the BaL_2 unit there are two long Ba–anionic O interactions, compared to one short interaction and one non-co-ordinated phosphinate group [Ba(1) · · · O(4) 3.39 Å] for each metal centre of Ba_2L_4. Also noteworthy is the presence of aromatic π-stacking interactions between different ligands in the dinuclear fragment. The water molecule in each asymmetric unit forms an O–H · · · O hydrogen bond to the phosphinate oxygen atom O(5) of the mononuclear BaL_2 unit, with a separation between the two oxygen atoms of 2.71 Å.

Barium(II) commonly forms nine- or ten-co-ordinate complexes with multidentate nitrogen- or oxygen-donor ligands, especially if they carry a negative charge.[23] The comparison between the barium(II) and lead(II) structures is interesting, as the charges are the same and the ionic radii (1.35 and 1.20 Å respectively) are comparable: the lower co-ordination numbers and softer donor sets commonly seen for Pb^{II} presumably reflect the presence of a lone pair of valence electrons in the co-ordination sphere. The co-ordination geometry about Ba(2), in the mononuclear unit BaL_2, may be approximately described as a bicapped square prism, with the oxygen atoms as the caps and the square planes N(112), N(92), N(12B), N(10A) and N(11C), N(92A), N(121), N(101). The irregular nine-co-ordination in the Ba_2L_2 unit does not obviously correspond to any of the simple limiting cases of nine-co-ordinate geometries.

Conclusion

The anion $[L]^-$ affords a surprising diversity of structures, exhibiting a variety of different co-ordination modes, in its complexes with non-transition-metal ions: N_2, N_4 and N_4O modes have all arisen. We have seen how $[L]^-$ can give both one-dimensional helicates when acting as a bridge between two metal ions and discrete mononuclear complexes when all donor atoms bind to the same metal ion. In this respect it is similar to

Table 6 Selected bond lengths (Å) and angles (°) for $[(BaL_2)_3]\cdot 6MeCN\cdot 2H_2O$

Ba(1)–O(2A)	2.730(6)	Ba(1)–N(21)	2.946(9)
Ba(1)–N(72)	2.869(8)	Ba(1)–N(61)	3.043(8)
Ba(1)–N(12)	2.871(9)	Ba(1)–N(41)	3.055(9)
Ba(1)–N(52)	2.872(9)	Ba(1)–N(81)	3.088(8)
Ba(1)–N(32)	2.914(8)		
Ba(2)–N(112)	2.852(8)	Ba(2)–N(121)	3.062(8)
Ba(2)–O(6)	3.140(7)	Ba(2)–N(101)	3.055(9)
Ba(2)–N(92)	2.870(8)		
O(2A)–Ba(1)–N(72)	128.8(2)	N(52)–Ba(1)–N(61)	53.7(3)
O(2A)–Ba(1)–N(12)	80.8(2)	N(32)–Ba(1)–N(61)	69.9(2)
N(72)–Ba(1)–N(12)	115.3(3)	N(21)–Ba(1)–N(61)	164.9(2)
O(2A)–Ba(1)–N(52)	92.7(2)	O(2A)–Ba(1)–N(41)	151.8(2)
N(72)–Ba(1)–N(52)	70.9(2)	N(72)–Ba(1)–N(41)	66.7(2)
N(12)–Ba(1)–N(52)	173.0(2)	N(12)–Ba(1)–N(41)	116.1(2)
O(2A)–Ba(1)–N(32)	119.3(2)	N(52)–Ba(1)–N(41)	68.9(2)
N(72)–Ba(1)–N(32)	111.8(2)	N(32)–Ba(1)–N(41)	54.9(2)
N(12)–Ba(1)–N(32)	69.6(2)	N(21)–Ba(1)–N(41)	128.4(2)
N(52)–Ba(1)–N(32)	111.9(2)	N(61)–Ba(1)–N(41)	66.7(2)
O(2A)–Ba(1)–N(21)	79.6(2)	O(2A)–Ba(1)–N(81)	144.8(2)
N(72)–Ba(1)–N(21)	73.2(2)	N(72)–Ba(1)–N(81)	54.7(2)
N(12)–Ba(1)–N(21)	55.9(3)	N(12)–Ba(1)–N(81)	70.0(2)
N(52)–Ba(1)–N(21)	125.8(3)	N(52)–Ba(1)–N(81)	117.1(2)
N(32)–Ba(1)–N(21)	118.5(3)	N(32)–Ba(1)–N(81)	68.5(2)
O(2A)–Ba(1)–N(61)	85.3(2)	N(21)–Ba(1)–N(81)	68.0(2)
N(72)–Ba(1)–N(61)	116.7(2)	N(61)–Ba(1)–N(81)	126.8(2)
N(12)–Ba(1)–N(61)	122.5(3)	N(41)–Ba(1)–N(81)	62.7(2)
N(112)–Ba(2)–N(92)	66.7(2)	N(101)–Ba(2)–N(121)	107.4(2)
N(112A)–Ba(2)–N(92)	113.3(2)	N(112)–Ba(2)–O(6A)	123.7(2)
N(112)–Ba(2)–N(101A)	73.9(2)	N(92)–Ba(2)–O(6A)	122.5(2)
N(112A)–Ba(2)–N(101A)	106.1(2)	N(101)–Ba(2)–O(6A)	70.9(2)
N(92)–Ba(2)–N(101A)	126.4(2)	N(121)–Ba(2)–O(6A)	72.4(2)
N(92A)–Ba(2)–N(101A)	53.6(2)	N(112)–Ba(2)–O(6)	56.3(2)
N(112)–Ba(2)–N(121A)	125.5(2)	N(92)–Ba(2)–O(6)	57.5(2)
N(92)–Ba(2)–N(121A)	71.4(2)	N(92A)–Ba(2)–O(6)	122.5(2)
N(112)–Ba(2)–N(121)	54.5(2)	N(101)–Ba(2)–O(6)	109.1(2)
N(92)–Ba(2)–N(121)	108.6(2)	N(121)–Ba(2)–O(6)	107.6(2)
N(101A)–Ba(2)–N(121)	72.6(2)		

other versatile ligands such as 2,2′:6′,2″:6″,2‴-quaterpyridine. In three of the four structures complex hydrogen-bonding networks involving solvent molecules help to stabilise the crystal lattice. Depending on the electronic demands of the metal centre, the anionic phosphinate oxygen atom may be pendant or may co-ordinate, giving $[L]^-$ the option of behaving as a solely N-donor or mixed N,O-donor ligand. We are currently attempting to extend its co-ordination chemistry to transition metals and lanthanides.

Acknowledgements

We thank the EPSRC for a grant to purchase the diffractometer.

References

1 E. C. Constable, *Prog. Inorg. Chem.*, 1994, **42**, 67; D. Philp and J. F. Stoddart, *Angew. Chem., Int. Ed. Engl.*, 1996, **35**, 1155; D. S. Lawrence, T. Jiang and M. Levett, *Chem. Rev.*, 1995, **95**, 2229; D. B. Amabilino and J. F. Stoddart, *Chem. Rev.*, 1995, **95**, 2725; J.-M. Lehn, *Supramolecular Chemistry*, VCH, Weinheim, 1995.

2 R. W. Saalfrank, R. Harbig, J. Nachtrab, W. Bauer, K.-P. Zeller, D. Stalke and M. Teichert, *Chem. Eur. J.*, 1996, **2**, 1363; L. J. Charbonniere, G. Bernardinelli, C. Piguet, A. M. Sargeson and A. F. Williams, *J. Chem. Soc., Chem. Commun.*, 1994, 1419; C. Piguet, G. Bernardinelli, B. Bocquet, O. Schaad and A. F. Williams, *Inorg. Chem.*, 1994, **33**, 4112; A. Bilyk, M. M. Harding, P. Turner and P. W. Hambley, *J. Chem. Soc., Dalton Trans.*, 1994, 2783; A. Juris and R. Ziessel, *Inorg. Chim. Acta*, 1994, **225**, 251; C. O. Dietrich-Buchecker, J.-P. Sauvage, A. De Cian and J. Fischer, *J. Chem. Soc., Chem. Commun.*, 1994, 2231; E. C. Constable, M. J. Hannon, A. J. Edwards and P. R. Raithby, *J. Chem. Soc., Dalton Trans.*, 1994, 2669; A. F. Williams, C. Piguet and G. Bernardinelli, *Angew. Chem., Int. Ed. Engl.*, 1991, **30**, 1490; M. T. Youinou, R. Ziessel and J.-M. Lehn, *Inorg. Chem.*, 1991, **30**, 2144.

3 S. van Wallandael, M. W. Perkovic and D. P. Rillema, *Inorg. Chim. Acta*, 1993, **213**, 253; M. Haga, T. Ano, K. Kano and S. Yamabe, *Inorg. Chem.*, 1991, **30**, 3843.

4 K. T. Potts, M. Keshavarz-K, F. S. Tham, H. D. Abruña and C. R. Arana, *Inorg. Chem.*, 1993, **32**, 4422; E. C. Constable, M. J. Hannon, A. Martin, P. R. Raithby and D. A. Tocher, *Polyhedron*, 1992, **11**, 2967.

5 S.-M. Yang, K.-K. Cheung and C.-M. Che, *J. Chem. Soc., Dalton Trans.*, 1993, 3515; C.-W. Chan, C.-M. Che and S.-M. Peng, *Polyhedron*, 1993, **12**, 2169; E. C. Constable, S. M. Elder, J. Healy, M. D. Ward and D. A. Tocher, *J. Am. Chem. Soc.*, 1990, **112**, 4590; E. C. Constable, S. M. Elder, J. Healy and D. A. Tocher, *J. Chem. Soc., Dalton Trans.*, 1990, 1669; E. C. Constable, S. M. Elder and D. A. Tocher, *Polyhedron*, 1992, **11**, 1337.

6 Y. Yao, M. W. Perkovic, D. P. Rillema and C. Woods, *Inorg. Chem.*, 1992, **31**, 3956; J.-M. Lehn, J.-P. Sauvage, J. Simon, R. Ziessel, C. Piccini-Leopardi, G. Germain, J.-P. Declerq and M. van Meersche, *Nouv. J. Chim.*, 1983, **7**, 413.

7 A. J. Amoroso, A. M. Cargill Thompson, J. C. Jeffery, P. L. Jones, J. A. McCleverty and M. D. Ward, *J. Chem. Soc., Chem. Commun.*, 1994, 2751; H. Brunner and T. Scheck, *Chem. Ber.*, 1992, **125**, 701; Y. Lin and S. A. Lang, *J. Heterocycl. Chem.*, 1977, **14**, 345.

8 P. L. Jones, A. J. Amoroso, J. C. Jeffery, J. A. McCleverty, E. Psillakis, L. H. Rees and M. D. Ward, *Inorg. Chem.*, 1997, **36**, 10.

9 SHELXTL 5.03 program system, Siemens Analytical X-Ray Instruments, Madison, WI, 1995; Software package for use with the SMART diffractometer, Siemens Analytical X-Ray Instruments, Madison, WI, 1995.

10 V. S. Joshi, V. K. Kale, K. M. Sathe, A. Sarkar, S. S. Tavale and C. G. Suresh, *Organometallics*, 1991, **10**, 2898.

11 S. Folkert, C. D. Bryan, A. W. Cordes, P. Tharmaraj and V. Chandrasekhar, *Acta Crystallogr., Sect. C*, 1995, **34**, 2493.

12 A. J. Amoroso, J. C. Jeffery, P. L. Jones, J. A. McCleverty, P. Thornton and M. D. Ward, *Angew. Chem., Int. Ed. Engl.*, 1995, **34**, 1443; A. J. Amoroso, J. C. Jeffery, P. L. Jones, J. A. McCleverty, L. Rees, A. L. Rheingold, Y. Sun, J. Takats, S. Trofimenko, M. D. Ward and G. P. A. Yapp, *J. Chem. Soc., Chem. Commun.*, 1995, 1881; D. A. Bardwell, J. C. Jeffery, P. L. Jones, J. A. McCleverty and M. D. Ward, *J. Chem. Soc., Dalton Trans.*, 1995, 2921.

13 A. Marquis-Rigault, J. Dupont-Gervais, A. van Dorsselaer and J.-M. Lehn, *Chem. Eur. J.*, 1996, **2**, 1395.

14 E. C. Constable, M. J. Hannon and D. A. Tocher, *J. Chem. Soc., Dalton Trans.*, 1993, 1883.

15 A. J. Amoroso, J. C. Jeffery, P. L. Jones, J. A. McCleverty, E. Psillakis and M. D. Ward, *J. Chem. Soc., Chem. Commun.*, 1995, 1175.

16 P. L. Jones, K. L. V. Mann, J. C. Jeffery, J. A. McCleverty and M. D. Ward, *Polyhedron*, in the press.

17 G. Ferguson, M. C. Jennings, F. J. Lalor and C. Shanahan, *Acta Crystallogr., Sect. C*, 1991, **47**, 2079; A. H. Cowley, R. L. Geerts, C. M. Nunn and S. Trofimenko, *J. Organomet. Chem.*, 1989, **365**, 19.

18 O. J. Gelling, F. van Bolhuis and B. L. Feringa, *J. Chem. Soc., Chem. Commun.*, 1991, 917; O. J. Gelling and B. L. Feringa, *J. Am. Chem. Soc.*, 1990, **112**, 7599; T. Suzuki, H. Kotsuki, K. Isobe, N. Moriya, Y. Nakagawa and M. Ochi, *Inorg. Chem.*, 1995, **34**, 530; Y. Dai, T. J. Katz and D. A. Nichols, *Angew. Chem., Int. Ed. Engl.*, 1996, **35**, 2109.

19 R. F. Carina, G. Bernardinelli and A. F. Williams, *Angew. Chem., Int. Ed. Engl.*, 1993, **32**, 1463; H. Hartl and F. Mahdjour-Hassan-Abadi, *Angew. Chem., Int. Ed. Engl.*, 1994, **33**, 1841; I. A. Tikhonova, F. M. Dolgushin, A. I. Yanovsky, Y. T. Struchkov, A. N. Gavrilova, L. N. Saitkulova, E. S. Shubina, L. M. Epstein, G. G. Furin and V. B. Shur, *J. Organomet. Chem.*, 1996, **508**, 271.

20 E. C. Constable, A. M. W. Cargill Thompson, P. Harveson, L. Macko and M. Zehnder, *Chem. Eur. J.*, 1995, **1**, 360; E. C. Constable and A. M. W. Cargill Thompson, *J. Chem. Soc., Dalton Trans.*, 1992, 3467.

21 D. L. Reger, M. F. Huff, A. L. Rheingold and B. S. Haggerty, *J. Am. Chem. Soc.*, 1992, **114**, 579.

22 A. J. Amoroso, J. C. Jeffery, P. L. Jones, J. A. McCleverty and M. D. Ward, *Polyhedron*, 1996, **15**, 2023.

23 N. S. Poonia and A. V. Bajaj, *Chem. Rev.*, 1979, **79**, 389; D. E. Fenton, *Comprehensive Coordination Chemistry*, eds. G. Wilkinson, R. D. Gillard and J. A. McCleverty, Pergamon, Oxford, 1987, vol. 3, p. 1.

Received 21*st January* 1997; *Paper* 7/00475C